

OPEN ACCESS

EDITED BY Xinmai Yang, University of Kansas, United States

REVIEWED BY
Janggun Jo,
University of Michigan, United States
Juanjuan Gu,
Philips NA, United States

*CORRESPONDENCE
Rodney Macedo,

rodney_macedo@hotmail.com
Chandan Guha,
cquhamd@gmail.com

RECEIVED 22 April 2025 ACCEPTED 01 August 2025 PUBLISHED 02 September 2025

CITATION

Schumacher MM, Gutierrez Chavez C, Malachowska B, Pandey S, Tchaikovskaya T, Singh S, Barry S, Macedo R and Guha C (2025) Enhancing tumoricidal effects of radiation therapy with low-intensity focused ultrasound in murine breast cancers. *Front. Acoust.* 3:1616297. doi: 10.3389/facou.2025.1616297

COPYRIGHT

© 2025 Schumacher, Gutierrez Chavez, Malachowska, Pandey, Tchaikovskaya, Singh, Barry, Macedo and Guha. This is an openaccess article distributed under the terms of the Creative Commons Attribution License (CC BY). The use, distribution or reproduction in other forums is permitted, provided the original author(s) and the copyright owner(s) are credited and that the original publication in this journal is cited, in accordance with accepted academic practice. No use, distribution or reproduction is permitted which does not comply with these terms.

Enhancing tumoricidal effects of radiation therapy with low-intensity focused ultrasound in murine breast cancers

Michelle Marie Schumacher^{1,2}, Claudia Gutierrez Chavez¹, Beata Malachowska¹, Sanjay Pandey¹, Tatyana Tchaikovskaya¹, Saurabh Singh¹, Steve Barry¹, Rodney Macedo^{1*} and Chandan Guha^{1,2*}

¹Department of Radiation Oncology, Albert Einstein College of Medicine, Montefiore Medical Center, Bronx, NY, United States, ²Department of Pathology, Albert Einstein College of Medicine, Bronx, NY, United States

Introduction: Focal cancer therapies fail to cure metastatic disease. Our prior studies indicated that Low Intensity Focused Ultrasound (LOFU) boosts antitumoral immunity in murine melanoma and prostate cancer. We hypothesized that LOFU, combined with radiation therapy (RT), could stimulate an immunogenic tumor microenvironment (TME) in murine breast cancers, potentially acting as an in-situ vaccine.

Methods: We evaluated LOFU \pm RT in TSA and E0771 breast cancer models in BALB/c and C57BL/6 mice, respectively, and measured intra-tumoral temperatures and gene expression to assess acoustic thermal stress using quantitative RT-PCR.

Results: Flow cytometry and gene expression showed that LOFU induced unfolded protein response pathway and heat shock protein RNA. LOFU modified the immune contexture in the TME of both tumor models, notably by increasing CD8+ T cell infiltration, including anti-gp70 CD8+ T cells, and reducing the RT-induced regulatory T cell response in TSA tumors.

Discussion: LOFU, as a non-ablative therapeutic, primes the TME and augments control of murine breast cancers by inducing tumor-specific adaptive immune responses.

KEYWORDS

Low Intensity Focused Ultrasound (LOFU), radiotherapy, tumor microenvironment, immunomodulation, CD8-positive T-Lymphocytes

1 Introduction

Breast cancer remains a significant health concern, with estimates suggesting that 1 in 8 American women will be diagnosed with invasive breast cancer in their lifetime (Society, 2022). Alarmingly, about 30% of these early-stage diagnoses progress to metastatic disease (O'Shaughnessy, 2005). While traditional localized treatments like surgery and radiation therapy (RT) effectively eradicate primary tumors, their efficacy in preventing metastasis is limited. This limitation is partly attributed to the infrequent occurrence of an abscopal effect following localized treatments and cancer's adeptness at immune evasion (Hu et al., 2017; Mole, 1953).

Emerging evidence suggests that targeting cancer's cytoprotective mechanisms, specifically the Unfolded Protein Response (UPR), could enhance tumor immunogenicity (Fabian et al., 2021). Intensifying the duration and degree of proteostatic stress on cancer cells may disrupt their survival mechanisms, particularly when homeostasis restoration fails (Fribley et al., 2009). Our research leverages this strategy through the development of Low Intensity Focused Ultrasound (LOFU) therapy, a non-ablative treatment inducing acoustic stress in cancer cells. LOFU has demonstrated promising results in immune priming in murine models of melanoma, prostate, and breast cancer (Bandyopadhyay et al., 2016; Saha et al., 2014; Skalina et al., 2019).

In this study, we have combined LOFU with RT, aiming to amplify both local and systemic tumoricidal effects in two murine breast cancer models, TSA and E0771. While the effects of LOFU + RT on the immune response in prostate cancer have been documented, particularly in the spleen (Skalina et al., 2019), its impact on the immune landscape of the Tumor Microenvironment (TME) in breast cancer warrants further investigation.

Our hypothesis is that non-ablative LOFU pre-treatment, as an immune priming therapy, followed by radiation, will significantly modify the immune contexture of the murine breast TME. We anticipate that this approach will facilitate the infiltration of activated anti-tumor immune cells, increasing the ratio of tumor-specific CD8+T cells to regulatory T cells (Tregs), thereby enhancing tumor control. Initial experiments involved optimizing LOFU parameters using our in-house ultrasound system, APTx, to induce maximal proteostatic stress in the TME. We then evaluated the effects of prolonged stress from LOFU, alone and in combination with RT, on immunogenic modulation and activation of the Immunogenic Cell Death (ICD) pathway in tumor cells.

Furthermore, we explored the anti-tumoral response to LOFU \pm RT in orthotopic breast tumor models, monitoring tumor growth progression and overall survival. This included survival studies in athymic mice and a wild-type dual tumor model to evaluate systemic anti-tumoral immunity and the regression of distant untreated tumors. Immunophenotyping of primary tumors post-treatment provided valuable insights into treatment effects and the role of the adaptive immune response in tumor control. These preclinical studies form a foundation for the development of combination immunotherapy and focal ablative therapies, targeting systemic control of metastatic cancer.

Abbreviations: APTx, Acoustic Priming Therapy; Atf6, Activating Transcription Factor 6; CRL, Charles River Laboratories; CTLA-4, Cytotoxic T Lymphocyte Antigen 4; DAMP, Damage Associated Molecular Pattern; DC, Dendritic Cell; ER, Endoplasmic Reticulum; HIFU, High Intensity Focused Ultrasound; HMGB1, High-Mobility Group Box 1 Protein; HSP, Heat Shock Protein; ICD, Immunogenic Cell Death; IFNy, Interferon-Gamma; LOFU, Low-Intensity Focused Ultrasound; MDSC, Myeloid-Derived Suppressor Cells; MHC-I, Major Histocompatibility Class I; N, Number of Mice Per Group; NT, Non-Treated; PD-1, Programmed Cell Death 1; PD-L1, Programmed Cell Death 1 Ligand; PERK, Pancreatic Er Kinase (Pkr)-Like Er Kinase; RFP, Red Fluorescent Protein; RT, Radiation Therapy; SSD, Extended Source To Surface Distance; Tem, T Effector Memory; TGF-β, Transforming Growth Factor-B; TME, Tumor Microenvironment; TNFa, Tumor Necrosis Factor Alpha; Treg, Regulatory T Cell; UPR, Unfolded Protein.

2 Materials and methods

2.1 Animals, tumor inoculation, and treatment group design

Female BALB/c, C57BL/6, and athymic nude mice (6–8 weeks old) were obtained from Charles River Laboratories (CRL). Before inducing orthotopic tumors, the mice were anesthetized under continuous inhaled 2% isoflurane in 2 L/min O2 using a Vetequip anesthesia system and hair was removed with an at home hair remover (Nair) from the abdominal area near the fourth inguinal mammary fat pad.

Tumors were induced using TSA (a gift from Silvia Formenti, Cornell) and E0771 cell lines (sourced from ATCC) under the same anesthesia regimen as above. For tumor induction, 0.1×10^6 TSA cells in 50 μ L were injected into BALB/c or athymic nude mice, and 0.5×10^6 E0771 cells in 50 μ L into C57BL/6 mice. In dual tumor studies, a secondary tumor was inoculated contralaterally, 3 days after the first. Mice were then randomized into treatment groups.

Study groups comprised non-treated controls, LOFU monotherapy, RT monotherapy, and LOFU + RT combination therapy, see supplemental methods for more details. For the majority of experiments, 5 mice were allocated to each group per experiment, with a total of ≥ 3 repeats. This design provides 80% statistical power to detect 2 standard deviation (SD) difference between group means. The exact number of mice used in each experimental group is specified in the corresponding figure legends.

All experimental procedures were conducted in accordance with protocols authorized by the Institutional Animal Care and Use Committee of Albert Einstein College of Medicine.

2.2 Animal treatment schema

Briefly, after tumor inoculation, tumors grew for about 11 days to become palpable and fall within an acceptable treatment diameter (\sim 4–6 mm). We then performed a regimen of three consecutive days of LOFU \pm RT. LOFU (240 W/cm²) was performed 2–4 h prior to a non-curative (sub-ablative) dose of X-ray orthovoltage (8Gy/or 10Gy/fraction). All animal treatments were performed under anesthesia. The mice were anesthetized under continuous inhaled 2% isoflurane in 2 L/min O2 using a Vetequip anesthesia system for ultrasound (<5 min/mouse) and irradiation (\sim 10 min/mouse) procedures.

2.3 Ultrasound treatment

The low-intensity focused ultrasound (LOFU) treatment was delivered using a dual frequency set-up consisting of 1.1 MHz and 250 KHz transducers, focused on the tumor target. All LOFU treatments were delivered with 100% duty cycle and no pulsing (PRF = 0) for a treatment time of 3 s.

Mice were anesthetized using isoflurane and placed supine on a custom-designed acoustic coupling platform. The tumor-bearing flank was covered in degassed ultrasound gel. The two ultrasound transducers (1.1 MHz and 250 kHz) were mounted coaxially, focusing at the tumor center. Tumor targeting was guided

visually and verified by external measurement. A continuous ultrasound signal was applied for 3 s using both transducers simultaneously. The platform ensured minimal animal movement and consistent beam alignment across animals.

Treatment intensities studied were 80 W/cm², 160 W/cm², and 240 W/cm². For all survival and immunophenotyping studies, 240 W/cm² LOFU was utilized.

2.4 Radiation treatment

Radiation treatment was performed using the Small Animal Radiation Research Platform (SARRP) (Xstrahl) to perform targeted tumor radiation of 8 or 10Gy at a dose rate of 3.3 Gy/min through a 10×10 mm collimator. Broad beam settings were 220 kVp and 13 mA, delivered through a 0.15 mm Cu filter. Beam SSD was 33 cm. The dose of 8Gy/3 was initially chosen because it, when in combination with the immunotherapy anti-CTLA4, had previously been shown to be effective in the regression of TSA tumors compared to other sub-ablative dosing such as 6Gy/5 + anti-CTLA4 (Liu et al., 2015).

2.5 Animal post-treatment observation and euthanasia

Following LOFU \pm RT treatment, mice were observed, with tumor volumes measured biweekly. Euthanasia, with 5% isoflurane overdose and secondary decapitation, followed predetermined endpoints. The day of euthanasia was noted for survival analysis. See supplemental methods for further details.

2.6 Tumor temperature measurements

For temperature studies, a type "T" 33-gauge hypodermic thermocouple (Omega Engineering) was placed into the center of the tumor tissue and temperature readings were acquired using a USB TC (Measurement Computing). Internal tumor temperature was recorded for 30 s before treatment, for the treatment duration, and until the temperature returned to baseline readings post-treatment using USB TC acquisition software (Measurement Computing). Mice treated for this study only received one dose of LOFU.

2.7 qRT- PCR

Five hours post a single LOFU treatment (80–240 W/cm²), mice were euthanized, and tumors were harvested for qRT-PCR analysis. Tumor tissue was cut into 1 mm pieces and preserved in RNALater at −80°C. Tumor tissue was later homogenized using a manual homogenizer and RNA was extracted using the Monarch Total RNA Miniprep Kit (New England Biolabs), according to manufacturer specifications. qRT-PCR analysis was performed to identify relative gene expressions of various target genes. 2.5 μg of each RNA sample were reversed transcribed using SuperScript IV VILO master mix (ThermoFisher) according to manufacturer protocol and then diluted to 2 ng per microliter with 0.1XTE buffer, pH 8.0. Gene expression assays, designed for each target gene, were validated with

control mouse mammary gland cDNA. PCR reactions were run in triplicate on the Quant Studio 6 Flex, with melting curve analysis ensuring specificity. Relative gene expression was calculated using 2 (-dCT) method and log-transformed. Rps13 and B2m assays served as reference genes. See supplemental methods for additional details and Supplementary Table S1 for a list of qRT-PCR primer sequences.

2.8 HMGB1 release assay and T-Cell stimulation

TSA cells transfected with HMGB1-tagged RFP were procured as a gift of Silvia Formenti (Cornell) and utilized to determine the relative release of HMGB1 after LOFU treatment. 2 × 106 HMGB1-tagged RFP cells per treatment condition were collected and pelleted down into a PCR tube (ThermoFisher) and placed in the focal zone of the APTx surrounding by ultrasound gel for LOFU (240 W/cm²) treatment. After treatment, cells were seeded back into a 6-well plate (CORNING) for incubation. Following a time course of 6, 24, 48 and 72 h, conditioned media from the cell cultures was collected and relative fluorescence was detected with a SpectraMax M3 spectrophotometer (Molecular Devices) at excitation and emission wavelengths of 530 nm and 593 nm respectively using the SoftMax Pro software (Molecular Devices). HMGB1 release by the TSA cells was evaluated via the relative fluorescent insanity of the conditioned media at each timepoint after treatment. Treatment with 100uM oxaliplatin (Sigma-Aldrich) was utilized as a positive control.

2.9 Flow cytometry

Prior to staining, tissues were harvested and homogenized into a single cell suspension, see supplemental methods for tissue homogenization and staining protocols. When staining was complete, data acquisition was performed using the Cytek Aurora (Cytek Biosciences) and analysis was performed with FlowJo software (BD Biosciences).

2.10 T Cell stimulation

10 days post treatment, after obtaining a single cell suspension of tumor tissue, $4 \times 10^6/\text{mL}$ cells were collected and stimulated with a protocol, modified from Ai et al., for optimal T cell cytokine production (Ai et al., 2013). Homogenized cells from treated tumor tissue were incubated with 1uL/mL of GolgiPlug (BD Biosciences). Then, half of the samples were kept as unstimulated control, and the other half was stimulated with a cocktail 20 uL/mL of PMA/Ionomycin Cell Activation Cocktail (without Brefeldin A) (Biolegend) incubated at 37°C for 4–6 h prior to cell collection for flow cytometry staining. See Supplementary Table S4 for full details on the T cell stimulation flow cytometry antibody panel.

2.11 Statistical analysis

Data from the experiments were statistically analyzed using GraphPad Prism (Dotmatics) and STASTISTICA 13.1. ANOVAs

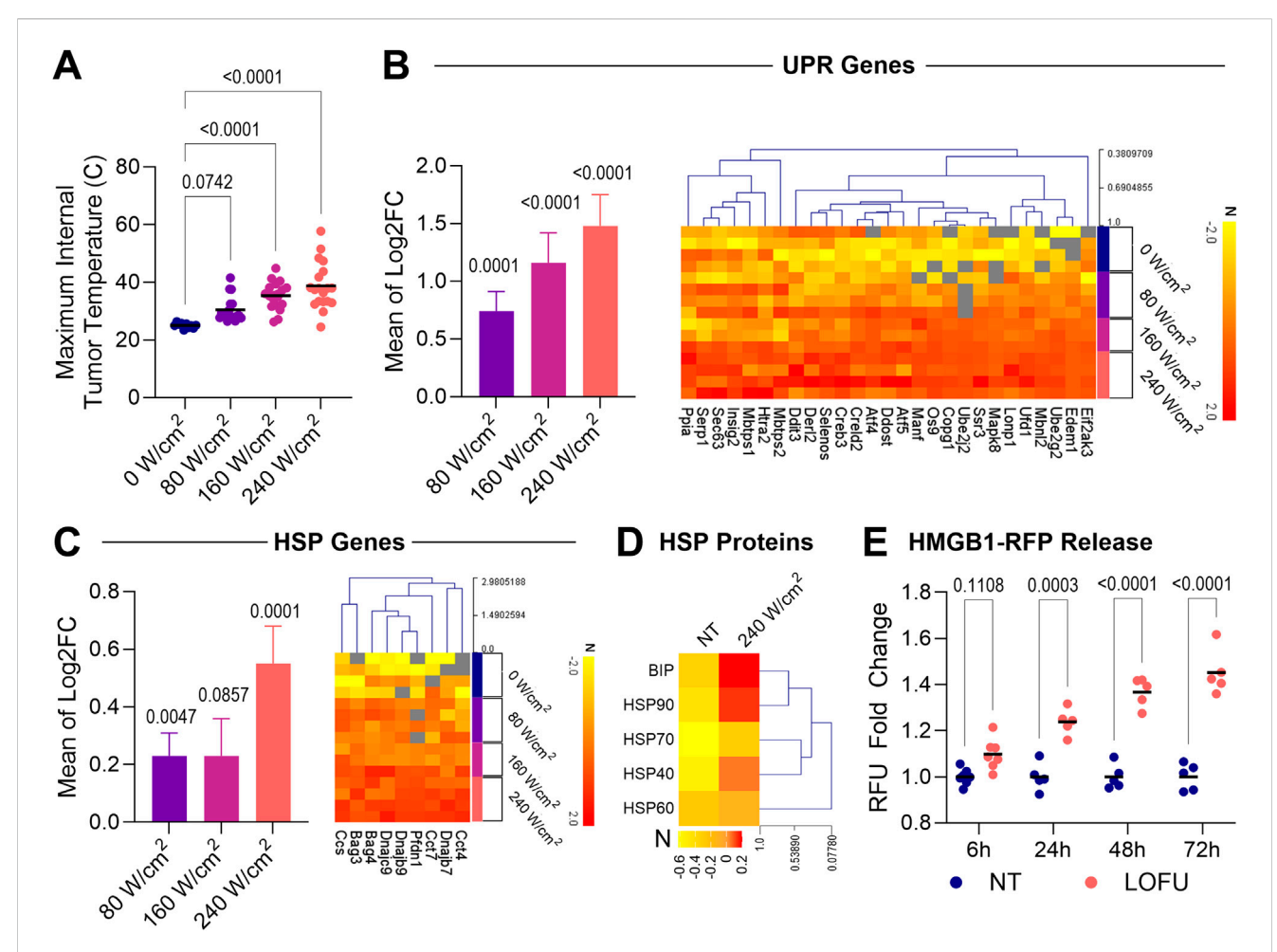


FIGURE 1 LOFU upregulates markers of ER stress and the unfolded protein response pathway in a dose dependent manner in TSA tumors. (A) Maximum internal temperature of TSA tumors after a single dose of LOFU at varying intensities; n = 10 for sham control mice and n = 18-19 mice for LOFU-treated groups. (B) UPR Genes. (Left) Gene expression of UPR genes in TSA tumors 5 h after LOFU treatment (80 W/cm², 160 W/cm², and 240 W/cm²) represented as the average fold change for all genes. (Right) Heatmaps of individual UPR genes significantly upregulated (p < 0.05) after treatment with 240 W/cm² LOFU. Unless otherwise indicated in associated gene expression heatmaps, n = 3 mice per treatment group. (C) HSP Genes. (Left) Gene expression of HSP genes in TSA tumors 5 h after LOFU treatment (80 W/cm², 160 W/cm², and 240 W/cm²) represented as the average fold change for all genes. (Right) Heatmaps of individual HSP genes significantly upregulated (p < 0.05) after treatment with 240 W/cm² LOFU. Unless otherwise indicated in associated gene expression heatmaps, n = 3 mice per treatment group. (D) Heatmap displaying the expression of HSPs on the surface of TSA tumors 24 h after three consecutive days of treatment with 240 W/cm² LOFU; n = 11-12 mice per group. (E) In vitro HMGB1 release time course, represented through the fold change of relative fluorescence units (RFU) in the conditioned media of TSA cells after treatment with 240 W/cm² LOFU; n = 5 or more individual biological cell replicates per treatment.

and t-tests were employed for endpoint comparisons, with post-hoc analysis using Tukey's test. Survival curves were analyzed via log-rank tests, and Cox proportional-hazards models estimated combined effects of treatments. Heatmaps were generated using MeV 4.8. Data are represented as mean \pm SEM, with p < 0.05 considered statistically significant. See supplemental methods for additional details.

3 Results

3.1 Dose response of acoustic cellular stress to LOFU

A key aspect differentiating LOFU from High-Intensity Focused Ultrasound (HIFU) is LOFU's ability to induce thermal and mechanical

stresses in tissues without causing ablation (Saha et al., 2014). It is therefore essential to ensure that the thermal acoustic stress from APTx is sufficient to elicit proteostatic stress and immunomodulation, but not so intense as to cause coagulative necrosis.

To optimize the LOFU parameters with APTx, we measured the maximum intra-tumoral temperatures during treatment, as shown in Figure 1A. We observed a dose-dependent increase in thermal effects with each LOFU intensity. Non-treated tumors (NT) maintained an average temperature around 25°C. In contrast, the average maximum internal tumor temperatures increased approximately 5°C with each escalating LOFU intensity (80 W/cm², 160 W/cm², and 240 W/cm²). At 240 W/cm², the average maximum internal tumor temperature reached approximately 38°C.

Subsequently, we investigated how varying LOFU intensities influenced proteostatic stress within tumor tissues. While previous

lab observations noted changes in key UPR components, a comprehensive understanding of transcriptomic regulation for various genes associated with this pathway was pending. By examining gene regulation following LOFU treatment, we aimed to establish a link between induced proteostatic stress and tumor cell immunomodulation. Specifically, we measured the mRNA expression of 62 genes associated with the UPR and 62 genes linked to Heat Shock Proteins (HSPs) 5 hours after LOFU treatment using qRT-PCR. We noted that both UPR and HSP gene expressions upregulated in a direct dose-dependent response to increasing LOFU intensities.

Remarkably, the most pronounced increase in the expression of cellular stress genes, without inducing tissue ablation, was observed following treatment with 240 W/cm² (Figures 1B,C; left). Thus, we selected 240 W/cm² as the standard intensity for LOFU treatments in the subsequent parts of our study. To illustrate the upregulation of individual genes within the HSP families and the UPR pathway, we generated heatmaps (Figures 1B,C; right). These heatmaps detailed individual genes that exhibited statistically significant upregulation (p < 0.05) following treatment with 240 W/cm² LOFU compared to non-treated tissue.

Having established the optimal LOFU treatment parameters for maximizing proteostatic stress in tumor cells, we next explored the immunomodulatory effects of this specific dose. Besides their role as chaperones, HSPs can act as Damage-Associated Molecular Patterns (DAMPs). When released from a cell, these complexes can induce Dendritic Cell (DC) activation and cross-presentation of peptide antigens to CD8⁺ T cells. Moreover, when applying a treatment regimen of three consecutive days of LOFU, we observed cytosolic HSPs, specifically BIP, HSP90, and HSP40, translocating to the cell surface within 24 h post-treatment, as depicted in Figure 1D. FACS gating strategies to identify CD45⁻tumor cells are shown in Supplementary Figure S1A. Percentages of cells positive for surface HSP expression are detailed in Supplementary Figure S1B.

Additionally, we utilized an expression system with TSA cells tagged with RFP-labeled High Mobility Group Box 1 (HMGB1) molecules. Our observations revealed that LOFU treatment progressively increased HMGB1 release from tumor cells *in vitro*, as illustrated in Figure 1E. Cells treated with 100uM Oxaliplatin served as a positive control for HMGB1 release (Supplementary Figure S1C).

3.2 Addition of RT to LOFU treatment improves immunogenicity of tumor cells

In our study, acknowledging the non-ablative nature of LOFU, we implemented a strategic approach of initial LOFU treatment for immune priming, followed by RT to boost ICD and promote tumor ablation. Our focus was on exploring the impact of three consecutive days of combined LOFU + RT treatment on the modulation of immunoregulatory expressions in tumor cells, as illustrated in Supplementary Figure S1D.

Achieving optimal anti-tumoral immunity necessitates a delicate balance between enhancing pro-immunogenic factors and suppressing pro-tumoral elements on the surface of tumor cells. Our results showed that RT stimulated an upregulation of various immunogenic markers. Particularly, it led to increased surface expression of CD40 and CD80 following treatments with

both RT alone and the combination of LOFU + RT. Interestingly, while RT alone induced the expression of calreticulin, an "eat-me" signal, the LOFU + RT combination resulted in diminished expression of CD47, a "do-not-eat-me" signal. This modulation potentially enhances the susceptibility of tumor cells to phagocytosis, offering a novel insight into the synergistic effects of combining LOFU and RT in cancer treatment.

3.3 LOFU augments the tumoricidal effects of RT via T cell mediated immunity

In our tumor growth survival studies, we focused on BALB/c mice with TSA tumors and C57BL/6 mice with E0771 tumors (Figure 2A). The results highlighted that adding LOFU to RT significantly improved survival compared to RT alone (Figures 2B,D). Notably, LOFU monotherapy was less effective in controlling tumors compared to the NT group.

Treatment responses in both TSA and E0771 cell lines are visually represented through spline and individual growth curves in Supplementary Figures S2A-D. These curves provide a clear depiction of tumor progression under different treatment conditions, shedding light on the efficacy of each approach. To add context and statistical relevance, the number of mice per group (n) is indicated alongside the individual tumor growth curves. This presentation method allows for a comprehensive understanding of the treatment impact across both cell lines, accentuating the similarities and differences in tumor responses. Further, we examined tumor burden at specific post-treatment intervals. Findings revealed that 38-40 days post-inoculation, all TSA tumor treatment groups had significantly lower tumor volumes compared to the NT group (Figure 2C, left). This difference became more pronounced at days 53-56, where the LOFU + RT combination treatment group exhibited a substantially lower tumor burden than the RT monotherapy group, indicating enhanced local tumor control (Figure 2C, right). In the E0771 tumor model, the superiority of LOFU + RT over RT monotherapy in controlling tumor growth was apparent earlier, around 30-32 days postinoculation (Figure 2E). These observations across different breast cancer models underscore the efficacy of the LOFU + RT combination therapy in achieving effective tumor control.

Additionally, survival benefits of LOFU + RT treatment were compared in both wild type and athymic mice bearing orthotopic TSA breast tumors. The survival advantage observed in wild type mice was not seen in athymic mice, lacking a functional T cell population (Figure 2F; Supplementary Figure S2E). This finding suggests that the tumoricidal effects of the LOFU + RT combination are significantly mediated by T cell activity.

In a dual tumor model using TSA, where only the primary tumor was treated, an abscopal effect was observed in the LOFU + RT group at 35 days post-inoculation (Supplementary Figure S2F). This treatment reduced the total tumor burden and affected both the treated primary and untreated secondary tumors. In contrast, RT monotherapy, while reducing the primary tumor burden, did not significantly impact the secondary untreated tumor. These results emphasize the systemic impact of LOFU + RT combination therapy, influencing untreated tumor sites, an effect not replicated by RT monotherapy.

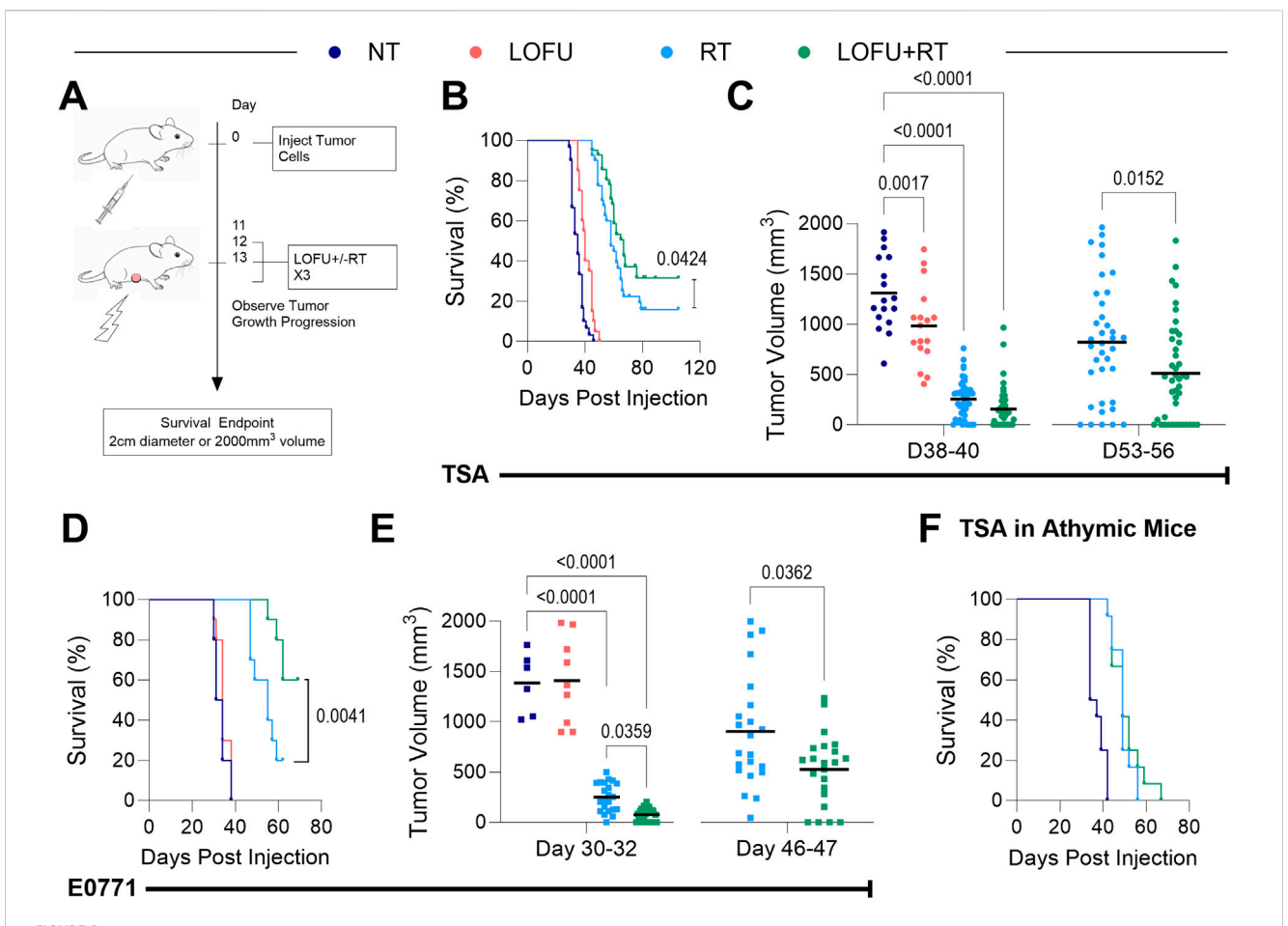


FIGURE 2
LOFU + RT promotes greater tumor control in a T-cell dependent manner. (A) Schema for survival studies with mice bearing TSA and
E0771 orthotopic breast tumors. (B) Survival curves for wild-type BALB/c mice bearing TSA tumors. (C) TSA tumor volumes for individual mice at
38–40 days (Left, n = 15–49 per treatment group), and 53–56 days post-inoculation (Right, n = 37–43 per treatment group). (D) Survival curves for wildtype C57BL/6 mice bearing E0771 tumors. (E) E0771 tumor volumes for individual mice at 30–32 days (Left, n = 6–23 per treatment group), and
46–47 days post-inoculation (Right, n = 23 per treatment group). (F) Survival of athymic TSA tumor-bearing mice; n = 12 mice per group. The number of
mice per group in each survival study is shown via individual tumor growth curves in Supplementary Figures S2B, D.

Our findings indicated that three consecutive days of treatment with sub-ablative doses (8Gy or 10Gy per fraction) did not sustain tumor eradication. However, integrating LOFU with these RT regimens significantly enhanced survival benefits. In the TSA survival study, combining LOFU with 8Gy per fraction provided a survival benefit comparable to 10Gy per fraction RT alone (Supplementary Figure S2G). This suggests LOFU's role in immune priming and potential in promoting tissue radiosensitization. The observation that 3 days of treatment with LOFU combined with 10Gy improved tumor control more than that of LOFU with 8Gy led us to adopt the higher dose strategy in subsequent immunophenotyping studies, allowing a deeper exploration of how this combination therapy enhances the immune response against tumors.

3.4 LOFU + RT improves the T cell response in the TME

Ten days after treatment, our investigation revealed no significant change in overall immune cell density within TSA or

E0771 tumor tissues, regardless of the treatment type, as illustrated in Figures 3A,B. However, a more detailed analysis into the specific immune subtypes present in the tumors showed treatment-dependent shifts in lymphoid and myeloid populations can be found in Figures 3C,D (Flow Cytometry gating strategies for lymphoid and myeloid populations can be found in Supplementary Figures S3A, B).

In our analysis of the myeloid compartment's subpopulations, detailed in Supplementary Figures S3C, D, we aimed to pinpoint the specific myeloid cells influenced by LOFU. The observed trends in changes among these subpopulations were largely consistent between TSA and E0771 tumors. A notable finding was that LOFU seemed to increase the percentage of macrophages within the myeloid compartment. However, this upregulation was not observed with the LOFU + RT combination, suggesting that the effect might be counteracted by RT. Particularly in TSA tumors, the LOFU-induced rise in myeloid cells could be largely attributed to an increase in macrophages.

Our findings within the lymphoid compartment show that RT, both as a monotherapy and in combination with LOFU, leads to an

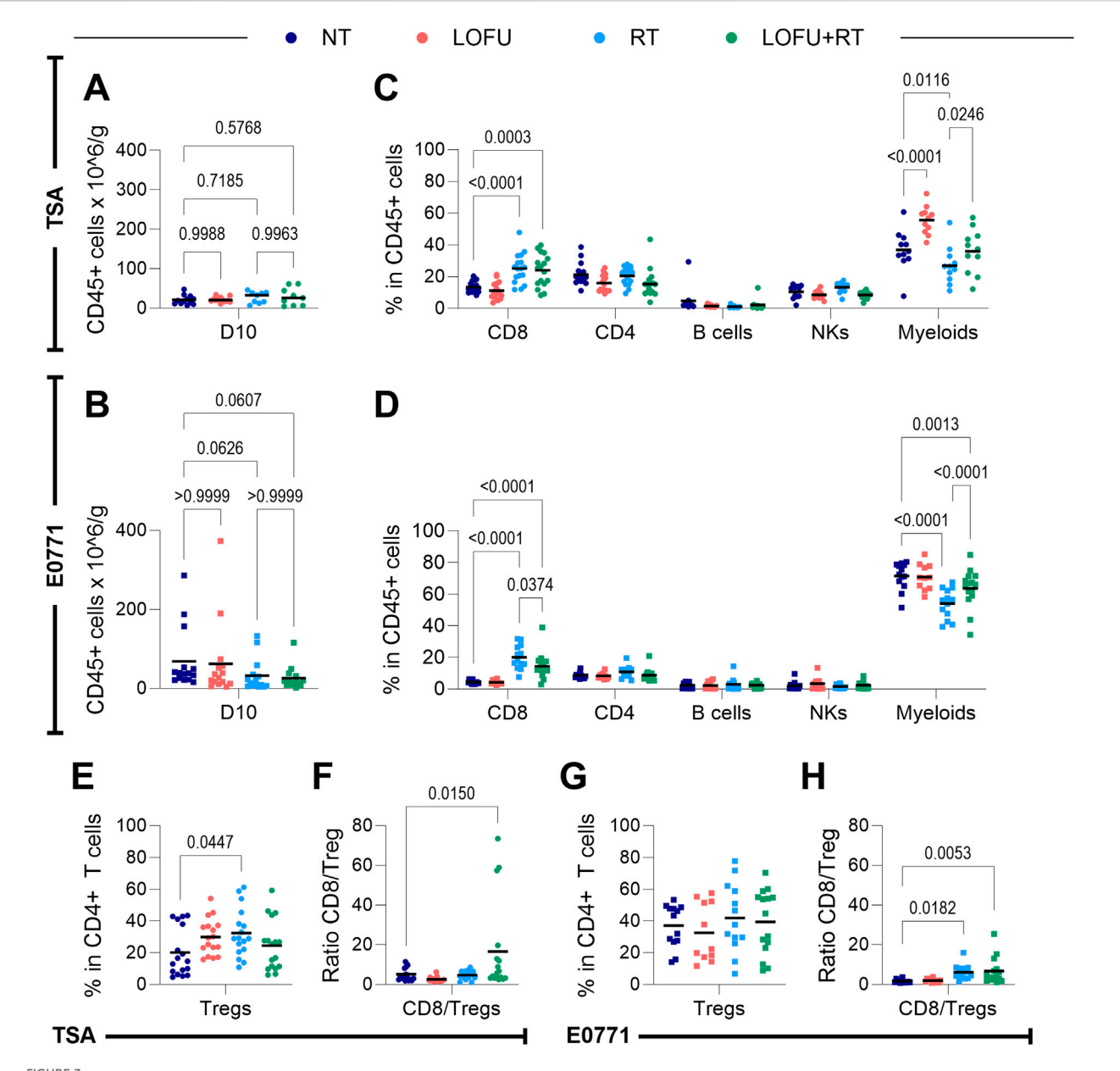


FIGURE 3
LOFU + RT alters the contexture of the tumor microenvironment but not overall immune cell density 10 days post treatment. (A,B) Density of immune cells in the TME of (A) TSA and (B) E0771 tumors; n = 9-15 mice per group. (C,D) Immune cell subpopulations present in the TME of (C) TSA and (D) E0771 tumors; n = 11-17 mice per group. (E) Percentage of Tregs present in the TME of TSA tumors; n = 17 mice per group. (F) Ratio of CD8* T cells to Tregs in TSA tumors; n = 11-17 mice per group. (G) Percentage of Tregs present in the TME of E0771 tumors; n = 11-15 mice per group. (H) Ratio of CD8* T cells to Tregs in E0771 tumors, n = 11-15 mice per group.

upregulation of CD8⁺ T cells within the TMEs of both TSA and E0771 tumors. Intriguingly, RT monotherapy results in a higher percentage of CD8⁺ T cells in the tumor compared to the LOFU + RT combination. Furthermore, although the overall quantity of CD4⁺ T cells in the tumors remains relatively consistent across treatment types, a noticeable shift is observed in the subtype composition of these CD4⁺ T cells. Systemic immune cell changes after treatment are shown in Supplementary Figures S3E-G and display the complex and nuanced effects of LOFU and RT treatments on the systemic immune system, extending beyond the immediate vicinity of the primary tumor to involve distant immune organs.

A unique alteration induced by RT in TSA tumors is the increased proportion of Tregs within the CD4⁺ T cell population following RT monotherapy. This effect is notably absent in the LOFU + RT group, as demonstrated in Figure 3E. As a result, there is a significant elevation in the CD8/Treg ratio within the TME in the LOFU + RT group compared to the NT group, a change not significantly mirrored in the RT monotherapy group (Figure 3F). While not reaching statistical significance in the E0771 model, there is an observable trend suggesting an RT-induced rise in the Treg population within the tumor (Figure 3G). Additionally, both RT and combination therapy groups exhibit higher CD8/Treg ratios

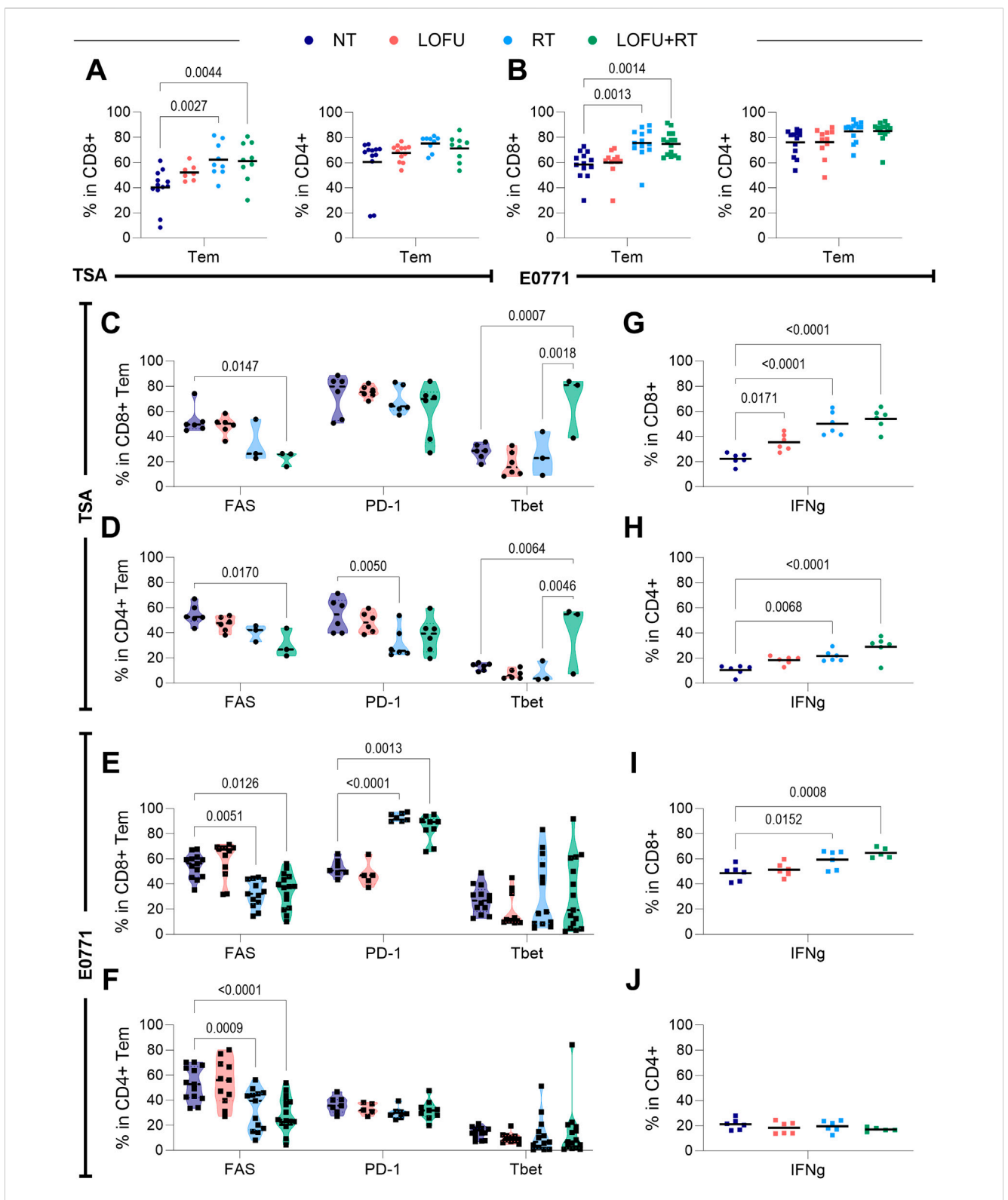


FIGURE 4
LOFU + RT improves the intratumoral T cell response. (A) Percentage of effector memory subtypes in TSA (Left) within CD8⁺ T cells and (Right) CD4⁺
T cells; n = 7-15 mice per group. (B) Percentage of effector memory subtypes in E0771 (Left) within CD8⁺ T cells and (Right) CD4⁺ T cells; n = 7-15 mice
per group. (C,D) Expression of T cell quality markers in (C) CD8⁺ and (D) CD4⁺ T cells in the TSA tumor microenvironment; n = 3-6 mice per group. (E,F)
Expression of T cell quality markers in (E) CD8⁺ and (F) CD4⁺T cells in the E0771 tumor microenvironment; n = 5-15 mice per group. (G,H)
Expression of IFN γ in (G) CD8⁺ and (H) CD4⁺ T cells in the TSA tumor microenvironment; n = 5-6 mice per group. (I,J) Expression of IFN γ in (I) CD8⁺ and (J) CD4⁺ T cells in the E0771 tumor microenvironment; n = 5-6 mice per group.

compared to NT in the E0771 model, with the combination group showing more pronounced significance (Figure 3H).

Given the insights from the athymic survival data (Figure 2F; Supplementary Figure S2E), which indicated that the efficacy of LOFU + RT treatment is partly mediated by T cells, we further explored the modulation of various T cell subsets. We particularly examined the increase in effector memory T cell (Tem) subtypes, characterized as CD44⁺ CD62L-, within both CD4⁺ and cytotoxic CD8⁺ T cell populations. These antigen-primed cells, capable of strategic positioning in both lymphoid and peripheral tissues, are crucial for efficiently executing their effector functions and initiating a comprehensive systemic immune response against tumors (Sallusto et al., 1999).

In both TSA and E0771 tumor models, we observed a radiation-induced enhancement in the proportion of Tem cells within the overall CD8⁺ T cell population. This increase was apparent in both the RT monotherapy and LOFU + RT groups, as depicted in Figures 4A,B; left. While there was no significant post-treatment increase in the Tem subtype within the CD4⁺ T cell population, a slight trend indicative of such an increase was noted (Figures 4A,B; right). These findings show the subtle yet impactful effects of radiation and the LOFU + RT combination therapy on different T cell subpopulations, particularly highlighting the significant role of Tem cells in the immune response within the TME.

Our analysis also extended to assessing the expression of immunomodulatory cell surface and cytoplasmic markers within the Tem cell populations. In TSA tumors, we discovered that the LOFU + RT combination not only influences the quantity but also enhances the quality of Tem cells in both CD4⁺ and CD8⁺ subsets (Figures 4C,D). This enhancement is reflected in the altered expression of specific cell surface markers. Notably, LOFU + RT reduces the percentage of both CD8⁺ and CD4⁺ Tem cells expressing FAS. Furthermore, there is an increase in the percentage of effector memory CD8⁺ cells expressing the transcription factor Tbet, both in comparison to NT and, interestingly, in comparison to RT monotherapy as well. This suggests that the combination treatment more effectively modulates these cell populations than RT alone.

Similarly, in E0771 tumors, as shown in Figures 4E,F, there is a consistent decrease in the expression of FAS in both CD8+ and CD4+ Tem cells following treatment with both RT and LOFU + RT. On the other hand, we observed an increase in the percentage of CD8+ Tem cells expressing PD-1 after treatments with RT and LOFU + RT. These finding suggest that targeted effects of LOFU + RT on Tem cell populations influence key immunomodulatory markers that may play a crucial role in the tumor's immune environment and response to therapy.

The activity of T cells in response to treatment can be effectively gauged by examining their secretion of cytokines, notably IFN γ and TNF α , following stimulation. In TSA tumors, as presented in Figures 4G,H, we observed a radiation-induced increase in IFN γ secretion in both CD8+ and CD4+ T cell populations following RT and LOFU + RT treatments. Notably, there is a trend indicating even greater IFN γ secretion in the LOFU + RT groups compared to RT alone. This suggests that the combination treatment may further enhance the cytokine response of T cells.

In E0771 tumors, illustrated in Figures 4I,J, we detected an upregulation in the expression of IFN γ in the CD8⁺ T cell population

post RT treatment when compared to the NT group. This increase was even more pronounced in the LOFU + RT group, indicating a trend towards enhanced cytokine expression with the combination therapy. However, it's important to note that no significant changes in IFN γ expression were observed in the effector memory CD4⁺ T cells in E0771 tumors based on treatment. These differential effects of RT and LOFU + RT on cytokine production by T cells within the TME shed light on the varying implications for the immune response to cancer therapies in these tumor models.

Comprehensive data detailing the percentage of CD8 $^{+}$ and CD4 $^{+}$ T cells expressing various markers, along with associated heatmaps, are thoroughly presented for both TSA and E0771 tumor types in Supplementary Figures S4A-D. This detailed analysis offers a deeper insight into the cellular responses to treatments. However, an intriguing observation emerges when comparing the effects on TNF α expression: Unlike the radiation-induced upregulation of IFN γ in comparison to the NT groups, a similar upregulation of TNF α is not observed in the LOFU + RT groups. This pattern holds true for both CD8 $^{+}$ and CD4 $^{+}$ T cell populations in both TSA and E0771 tumors, as shown in Supplementary Figures S4E-H.

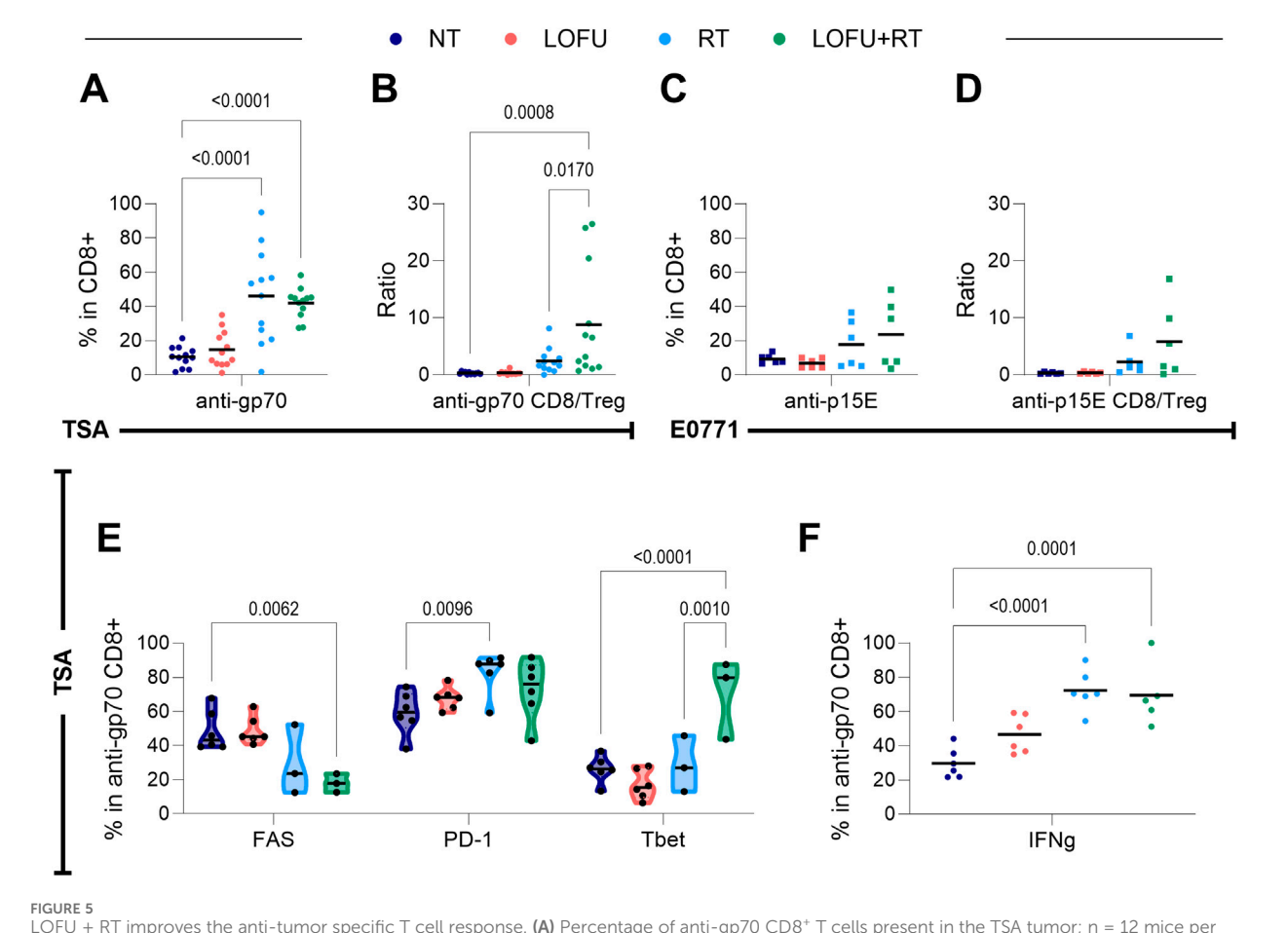
This discrepancy in the response of TNF α expression to radiation and combination therapy displays a distinct aspect of the immune response, underscoring the varied effects of LOFU + RT treatment. It suggests that while radiation alone can upregulate TNF α in T cells, the addition of LOFU may influence this cytokine response differently, indicating a nuanced interplay between these therapies in modulating the immune environment within tumors.

3.5 LOFU + RT improves the tumor-specific T cell response

To assess the adaptive immune response against cancer, we focused on evaluating T cells that recognize cancer-associated or specific antigens. In TSA tumors, the overexpressed gp70 epitope, a product of the murine gamma leukemia retrovirus (MuLV) presented on MHC-I H-2Ld molecules, was studied (Rosato et al., 2003). Additionally, we examined the p15E epitope, another gene product from MuLV presented on MHC-I H-2kb molecules. Using tetramer antibody staining for these MHC-Irestricted peptides, as previously performed by Rosato et al. (Rosato et al., 2003), we identified anti-gp70 CD8+ T cells in TSA tumors and anti-p15E CD8+ T cells in E0771 tumors. While gp70 is an established tumor-associated antigen (TAA) for TSA, p15E's status for E0771 is unknown, providing an opportunity to explore if LOFU treatment can induce p15E as a new antigen in this model. Gating strategies for these specific CD8+ T cells are shown in Supplementary Figure S5A.

In TSA tumors treated with RT or LOFU + RT, an increase in tumor-specific (anti-gp70) CD8⁺ T cell infiltration was observed (Figure 5A). Notably, the LOFU + RT treatment led to a significant rise in the anti-gp70 CD8/Treg ratio, surpassing both NT and RT-alone groups (Figure 5B). This indicates that combination therapy more effectively enhances the tumor-specific CD8⁺ T cell response relative to Tregs compared to RT alone.

In E0771 tumors, the LOFU + RT group demonstrated the highest percentage of anti-p15E CD8⁺ T cells, resulting in the greatest ratio of anti-p15E CD8⁺ T cells to Tregs (Figures 5C,D).



LOFU + RT improves the anti-tumor specific T cell response. (A) Percentage of anti-gp70 CD8+ T cells present in the TSA tumor; n = 12 mice per group. (B) Ratio of anti-gp70 CD8+ T cells to Tregs in the TSA tumor; n = 12 mice per group. (C) Percentage of anti-p15E CD8+ T cells present in the E0771 tumor; n = 6 mice per group. (D) Ratio of anti-p15E CD8+ T cells to Tregs in the E0771 tumor; n = 6 mice per group. (E) Expression of T cell quality markers in anti-gp70 CD8+ T cells within the TSA tumor microenvironment; n = 3-6 mice per group. (F) Expression of IFN γ in anti-gp70 CD8+ cells in the TSA tumor microenvironment; n = 5-6 mice.

However, this trend was not statistically significant. Given that p15E is not a recognized TAA for E0771 tumors, this finding suggests that anti-p15E CD8+ T cells may not serve as reliable markers for a tumor-specific immune response in the context of E0771 tumors. These results highlight the complexity of immune responses induced by different treatments, particularly the potential of LOFU + RT to enhance tumor-specific CD8+ T cell infiltration and modulate the immune landscape within these tumor models.

Moreover, our analysis revealed that in both TSA and E0771 tumors, the effector memory subset within the tumor specific CD8⁺ T cells remains unaffected by treatment type. This observation (Supplementary Figures S5B,C) indicates that treatments such as RT or LOFU + RT do not significantly alter the effector memory subgroup within these specific CD8⁺ T cells.

In TSA tumors, LOFU + RT treatment notably improved the quality of anti-gp70 CD8+ T cells (Figure 5E). This improvement is characterized by a decrease in the population of these cells expressing FAS and an increase in the percentage expressing Tbet. Importantly, the proportion of Tbet-expressing cells is higher in tumors treated with LOFU + RT compared to RT alone, suggesting a shift towards a Th1-biased adaptive immune

response. Additionally, there is an RT-induced increase in the population of these cells expressing PD-1.

Similar to the overall response of general CD8 $^{+}$ T cells to stimulation, TSA-specific CD8 $^{+}$ T cells exhibited an increase in IFN γ levels post-treatment with both RT and LOFU + RT (Figure 5F). This consistent increase in IFN γ suggests that these treatments enhance the functional capabilities of tumor-specific CD8 $^{+}$ T cells in TSA tumors. However, no noticeable change in TNF α expression was observed in anti-gp70 CD8 $^{+}$ T cells regardless of treatment type (Supplementary Figure S5D). Again it is evident that the multifaceted and targeted effects of LOFU + RT, specifically on tumor-specific T cell populations, are critical in shaping the immune response within the TME.

4 Discussion

Our observations indicate that increasing LOFU intensity not only raises the maximum temperature within the tumor, as shown in Figure 1A, but also escalates the cellular stress response in a dose-dependent manner (Figures 1B,C). This correlation between thermal

effects and LOFU dosage is linked to heightened expression of UPR and HSP genes within the tumor tissue.

The UPR is marked by three principal pathways mediated by ATF6, PERK, and IRE1α, each crucial in cellular cytoprotective mechanisms to restore homeostasis (McGrath et al., 2018). Analyzing gene expression within the TME 5 h post-LOFU treatment helped us gain insights into the specific UPR pathways activated by LOFU. Among the 62 UPR genes examined, 27 showed increased expression following 240 W/cm² LOFU treatment, spanning key pathways of the UPR (Figure 1B). Particularly, there was notable upregulation in genes linked to the PERK-ATF4 signaling pathway, including Eif2ak, which encodes for PERK. PERK is known for phosphorylating eIF2α, leading to a global attenuation of methionine-initiated translation, a component of the integrated stress response (Hetz et al., 2020). This shift towards non-canonical mRNA translation has been associated with the generation of MHC-I peptides (Apcher et al., 2022).

We found that HSP genes were generally upregulated following LOFU treatments (Figure 1C). HSPs, particularly HSP60, HSP70, and HSP90, are known for facilitating antigen cross-presentation to antigen-presenting cells (Tsan and Gao, 2009). This upregulation suggests that LOFU treatments effectively enhance the antigenicity of the cell. However, we observed that gene products predominantly upregulated in response to 240 W/cm² LOFU treatment belonged to the HSP40 family and other protein regulators, rather than HSP90 or HSP70 families. This finding indicates a specific response pathway activated by LOFU treatment.

While LOFU's categorization as either a type I or type II ICD inducer remains ambiguous due to its potential direct and indirect impacts on the ER, it offers a focal therapy advantage, targeting only the local tissue within the treatment area (Oslowski and Urano, 2011). LOFU alone appears to act as an ICD inducer, evident in HSP translocation to the cell surface and the upregulation of DAMP factors like HMGB1 release over time (Figures 1D,E), aligning with our previous findings in murine breast and prostate tumors (Skalina et al., 2019).

However, similar to certain Endoplasmic Reticulum (ER) stress-inducing drugs like tunicamycin, the mere induction of an ER stress response may not be sufficient for the associated calreticulin surface expression, a critical element of ICD (Peters and Raghavan, 2011). This seems to be the case with LOFU, as LOFU monotherapy does not induce calreticulin surface expression on tumor cells, while RT monotherapy does (Figure 3.4). Therefore, combining LOFU with RT aims to maximize cell stress and subsequent immune priming effects within the TME. Indeed, we find that adding RT to LOFU therapy enhances the expression of pro-immunogenic factors such as CD40 and CD80, while concurrently reducing the expression of the immune-suppressive marker CD47 on tumor cells (Supplementary Figure S1D). For optimal treatment of breast tumors, we propose a combination therapy of LOFU + RT.

Combining LOFU with RT significantly enhances tumor control in our TSA and E0771 tumor models (Figures 2B–D). However, this "cure," defined as tumor regression to a non-palpable size, is often transient, with tumors frequently recurring (Supplementary Figures S2A-D). While this combination therapy extends survival and controls tumor growth, it cannot be deemed curative, echoing a clinical challenge where approximately 15% of early-stage breast cancer patients experience local recurrence within 15 years (Sopik et al., 2016).

LOFU's role as a radiosensitizer is crucial, especially considering the clinical goal of maximizing tumor dosage while minimizing adverse effects on surrounding healthy tissue. For radio-tolerant patients, a 1% RT dose increase can improve the probability of tumor control by 1%–2%, while a dose reduction of 20% could virtually eliminate serious side effects in radiation-sensitive patients (Barnett et al., 2009). Our survival studies demonstrate that LOFU allows a 20% reduction in RT dosage while maintaining comparable tumor control to higher doses alone, potentially reducing serious side effects in radiation-sensitive patients (Supplementary Figure S2G).

The addition of LOFU to radiotherapy may also be important for launching a successful systemic anti-tumoral immune response. The dual tumor model study shows that LOFU + RT not only regresses the primary treated tumor but also exhibits an abscopal effect on a secondary non-treated tumor (Supplementary Figure S2F). This systemic response appears to be T cell-mediated, as suggested by parallel studies with TSA tumors in wild type and athymic mice (Figure 2F).

Immunophenotyping experiments, conducted 10 days post-treatment, shed light on the immune contexture of the TME. Despite radiation-induced upregulation of CD8+ T cells in TSA and E0771 tumors, an increase in Tregs was noted in irradiated TSA tumors (Figures 3C–E,G). While there have been reports supporting our findings that radiation treatment increases the Treg response (Liu et al., 2015), the addition of LOFU to RT does not increase the percentage of Tregs beyond NT levels. Excitingly, this translates to a significant increase in the CD8/Treg ratio of the combination-treated group compared to NT in both TSA and E0771 tumors (Figures 3F,H). This CD8/Treg ratio is clinically relevant in breast cancer, positively correlating with improved survival outcomes (Goda et al., 2022; Liu et al., 2011; Tavares et al., 2021). Overall, these findings suggest that LOFU reprograms the tumor immune microenvironment to support immune-activating pathways while suppressing immunoinhibiting pathways.

More in-depth analysis showed an upregulation of tumor-specific anti-gp70 CD8 $^{+}$ T cells in TSA tumors as well as the anti-gp70 CD8 $^{+}$ T cells/Treg ratio post-combination treatment (Figures 5A,B), affirming the tumor specificity of the adaptive immune response to LOFU + RT. Thus, the LOFU + RT combination leverages the immune system to target specific tumors, offering broad applicability across different tumor types. Further, the improved quality of the upregulated anti-gp70 CD8 $^{+}$ T cells through cell surface modulation suggests increased adaptive immunity and bolstered cytotoxicity against the tumor (Figures 5E,F).

Our study opens several avenues for further investigation. We aim to unravel the mechanisms underlying LOFU-induced proteostatic stress and its direct correlation with adaptive immune priming. Additionally, understanding the causes of LOFU + RT treatment failure, particularly the mechanisms behind tumor recurrence post-treatment, is crucial. We also plan to explore strategies to enhance the efficacy of LOFU + RT, potentially through the addition of anti-PD-1 therapy or surgical resection post-treatment. The role of myeloid cells within the TME post-LOFU + RT, especially the polarization of tumor-associated macrophages (TAMs), remains to be fully explored. These findings could provide deeper insights into the mechanisms of immune priming within the TME.

In conclusion, the findings of this study positions LOFU as a promising therapeutic tool capable of inducing significant cellular stress within the TME. When combined with non-ablative RT, LOFU + RT effectively alters the immune landscape of the breast

TME, promoting both a general and tumor-specific T cell response. This response is crucial for improving local tumor control, yet further research is needed to enhance its effectiveness and ensure long-lasting tumor control post-treatment.

Data availability statement

The original contributions presented in the study are included in the article/Supplementary Material, further inquiries can be directed to the corresponding authors.

Ethics statement

All animal experiments were conducted in accordance with protocols authorized by the Institutional Animal Care and Use Committee of Albert Einstein College of Medicine, protocol # 00001055.

Author contributions

MS: Funding acquisition, Writing - original draft, Software, Formal Analysis, Writing - review and editing, Visualization, Data curation, Methodology, Conceptualization, Validation, Resources, Project administration, Investigation. CGC: Writing - review and editing, Conceptualization, Data curation, Formal Analysis. Writing - original draft, Formal Analysis, Writing - review and editing. SP: Writing - review and editing, Conceptualization, Data curation. TT: Writing - review and editing, Writing - original draft. SS: Data curation, Writing - review and editing, Conceptualization. SB: Writing - original draft, Conceptualization, Writing - review and editing. RM: Formal Analysis, Data curation, Conceptualization, Writing - review and editing. CG: Project administration, Formal Analysis, Data curation, Validation, Visualization, Methodology, Conceptualization, Software, Funding acquisition, Writing - review and editing, Supervision, Writing - original draft, Resources, Investigation.

Funding

The author(s) declare that financial support was received for the research and/or publication of this article. This work was supported by the Training Program in Cellular and Molecular Biology and Genetics (T32GM007491). We would like to thank the Albert Einstein Cancer Center for their support (P30CA013330). We also thank the Albert

Einstein College of Medicine Flow Cytometry Core Facility (S10OD026833) for their assistance with this project.

Acknowledgments

We are grateful for the help of Wade Koba, who was instrumental in developing and troubleshooting the mouse treatment modalities required for this study. Thank you to Brett Bell and Justin Vercellino for their thoughtful edits of this manuscript. Data in this paper are from a thesis to be submitted in partial fulfillment of the requirements for the Degree of Doctor of Philosophy in the Biomedical Sciences, Albert Einstein College of Medicine (Schumacher, 2023).

Conflict of interest

CG is a consultant for Varian Medical Systems and the Focused Ultrasound Foundation. CG is co-founder of BioConvergent Health, LLC.

The remaining authors declare that the research was conducted in the absence of any commercial or financial relationships that could be construed as a potential conflict of interest.

Generative AI statement

The author(s) declare that no Generative AI was used in the creation of this manuscript.

Publisher's note

All claims expressed in this article are solely those of the authors and do not necessarily represent those of their affiliated organizations, or those of the publisher, the editors and the reviewers. Any product that may be evaluated in this article, or claim that may be made by its manufacturer, is not guaranteed or endorsed by the publisher.

Supplementary material

The Supplementary Material for this article can be found online at: https://www.frontiersin.org/articles/10.3389/facou.2025.1616297/full#supplementary-material

References

Ai, W., Li, H., Song, N., Li, L., and Chen, H. (2013). Optimal method to stimulate cytokine production and its use in immunotoxicity assessment. *Int. J. Environ. Res. Public Health* 10 (9), 3834–3842. doi:10.3390/ijerph10093834

Apcher, S., Tovar-Fernadez, M., Ducellier, S., Thermou, A., Nascimento, M., Sroka, E., et al. (2022). mRNA translation from an antigen presentation perspective: a tribute to the works of nilabh shastri. *Mol. Immunol.* 141 (2021), 305–308. doi:10.1016/j.molimm. 2021.12.010

Bandyopadhyay, S., Quinn, T. J., Scandiuzzi, L., Basu, I., Partanen, A., Tomé, W. A., et al. (2016). Low-Intensity focused ultrasound induces reversal of tumor-induced T cell tolerance and prevents immune escape. *J. Immunol.* 196 (4), 1964–1976. doi:10.4049/jimmunol. 1500541

Barnett, G. C., West, C. M. L., Dunning, A. M., Elliott, R. M., Coles, C. E., Pharoah, P. D. P., et al. (2009). Normal tissue reactions to radiotherapy: towards tailoring treatment dose by genotype. *Nat. Rev. Cancer* 9 (2), 134–142. doi:10.1038/nrc2587

Fabian, K. P., Wolfson, B., and Hodge, J. W. (2021). From immunogenic cell death to immunogenic modulation: select chemotherapy regimens induce a spectrum of immune-enhancing activities in the tumor microenvironment. *Front. Oncol.* 11, 728018. doi:10.3389/fonc.2021.728018

Fribley, A., Zhang, K., and Kaufman, R. J. (2009). Regulation of apoptosis by the unfolded protein response. *Methods Mol. Biol.* 559, 191–204. doi:10.1007/978-1-60327-017-5_14

Goda, N., Sasada, S., Shigematsu, H., Masumoto, N., Arihiro, K., Nishikawa, H., et al. (2022). The ratio of CD8 + lymphocytes to tumor-infiltrating suppressive FOXP3 + effector regulatory T cells is associated with treatment response in invasive breast cancer. *Discov. Oncol.* 13 (1), 27. doi:10.1007/s12672-022-00482-5

Hetz, C., Zhang, K., and Kaufman, R. J. (2020). Mechanisms, regulation and functions of the unfolded protein response. *Nat. Rev. Mol. Cell Biol.* 21 (8), 421–438. doi:10.1038/s41580-020-0250-z

Hu, Z. I., McArthur, H. L., and Ho, A. Y. (2017). The abscopal effect of radiation therapy: what is it and how can we use it in breast cancer? *Curr. Breast Cancer Rep.* 9 (1), 45–51. doi:10.1007/s12609-017-0234-y

Liu, F., Lang, R., Zhao, J., Zhang, X., Pringle, G. A., Fan, Y., et al. (2011). CD8+cytotoxic T cell and FOXP3+ regulatory T cell infiltration in relation to breast cancer survival and molecular subtypes. *Breast Cancer Res. Treat.* 130 (2), 645–655. doi:10. 1007/s10549-011-1647-3

Liu, S., Sun, X., Luo, J., Zhu, H., Yang, X., Guo, Q., et al. (2015). Effects of radiation on T regulatory cells in normal states and cancer: mechanisms and clinical implications. *Am. J. Cancer Res.* 5 (11), 3276–3285.

Mole, R. H. (1953). Whole body irradiation—radiobiology or medicine? *Br. J. Radiol.* 26 (305), 234–241. doi:10.1259/0007-1285-26-305-234

McGrath, E. P., Logue, S., Mnich, K., Deegan, S., Jäger, R., Gorman, A., et al. (2018). The unfolded protein response in breast cancer. *Cancers (Basel)* 10 (10), 344–21. doi:10. 3390/cancers10100344

Oslowski, C. M., and Urano, F. (2011). Measuring ER stress and the unfolded protein response using mammalian tissue culture system. *Methods Enzym.* 490, 71–92. doi:10. 1016/b978-0-12-385114-7.00004-0

O'Shaughnessy, J. (2005). Extending survival with chemotherapy in metastatic breast cancer. Oncologist 10 (S3), 20–29. doi:10.1634/theoncologist.10-90003-20

Peters, L. R., and Raghavan, M. (2011). Endoplasmic Reticulum calcium depletion impacts chaperone secretion, innate immunity, and phagocytic uptake of cells. *J. Immunol.* 187 (2), 919–931. doi:10.4049/JIMMUNOL.1100690

Rosato, A., Dalla Santa, S., Zoso, A., Giacomelli, S., Milan, G., Macino, B., et al. (2003). The cytotoxic T-lymphocyte response against a poorly immunogenic mammary adenocarcinoma is focused on a single immunodominant class I epitope derived from the gp70 Env product of an endogenous retrovirus. *Cancer Res.* 63 (9), 2158–2163.

Saha, S., Bhanja, P., Partanen, A., Zhang, W., Liu, L., Tomé, W. A., et al. (2014). Low intensity focused ultrasound (LOFU) modulates unfolded protein response and sensitizes prostate cancer to 17AAG. *Oncoscience* 1, 434–445. doi:10.18632/oncoscience.48

Sallusto, F., Lenig, D., Förster, R., Lipp, M., and Lanzavecchia, A. (1999). Two subsets of memory T lymphocytes with distinct homing potentials and effector functions. *Nature* 401, 708–712. doi:10.1038/44385

Schumacher, M. M. (2023). Enhancing tumoricidal effects of radiation therapy with low-intensity focused ultrasound in Murine breast cancers. Albert Einstein College of Medicine ProQuest Dissertations and Theses, 30997349. PhD diss.

Skalina, K. A., Singh, S., Chavez, C. G., Macian, F., and Guha, C. (2019). Low intensity focused ultrasound (LOFU)-mediated acoustic immune priming and ablative radiation therapy for *in situ* tumor vaccines. *Sci. Rep.* 9 (1), 15516–12. doi:10.1038/s41598-019-51332-4

Society, A. C. (2022). Breast Cancer Facts & Figures 2022-2024.

Sopik, V., Nofech-Mozes, S., Sun, P., and Narod, S. A. (2016). The relationship between local recurrence and death in early-stage breast cancer. *Breast Cancer Res. Treat.* 155 (1), 175–185. doi:10.1007/s10549-015-3666-y

Tavares, M. C., Sampaio, C. D., Lima, G. E., Andrade, V. P., Gonçalves, D. G., Macedo, M. P., et al. (2021). A high CD8 to FOXP3 ratio in the tumor stroma and expression of PTEN in tumor cells are associated with improved survival in non-metastatic triplenegative breast carcinoma. *BMC Cancer* 21 (1), 901–912. doi:10.1186/s12885-021-08636-4

Tsan, M.-F., and Gao, B. (2009). Heat shock proteins and immune system. *J. Leukoc. Biol.* 85 (6), 905–910. doi:10.1189/jlb.0109005